Loss of *O*-GlcNAc glycosylation in forebrain excitatory neurons induces neurodegeneration

Andrew C. Wang[a], Elizabeth H. Jensen[a], Jessica E. Rexach[a], Harry V. Vinters[b,c], and Linda C. Hsieh-Wilson[a,1]

[a]Division of Chemistry and Chemical Engineering, California Institute of Technology, Pasadena, CA 91125; [b]Division of Neuropathology, Department of Pathology and Laboratory Medicine, David Geffen School of Medicine at University of California, Los Angeles, CA 90095; and [c]Department of Neurology, David Geffen School of Medicine at University of California, Los Angeles, CA 90095

O-GlcNAc glycosylation (or *O*-GlcNAcylation) is a dynamic, inducible posttranslational modification found on proteins associated with neurodegenerative diseases such as α-synuclein, amyloid precursor protein, and tau. Deletion of the *O*-GlcNAc transferase (*ogt*) gene responsible for the modification causes early postnatal lethality in mice, complicating efforts to study *O*-GlcNAcylation in mature neurons and to understand its roles in disease. Here, we report that forebrain-specific loss of OGT in adult mice leads to progressive neurodegeneration, including widespread neuronal cell death, neuroinflammation, increased production of hyperphosphorylated tau and amyloidogenic Aβ-peptides, and memory deficits. Furthermore, we show that human cortical brain tissue from Alzheimer's disease patients has significantly reduced levels of OGT protein expression compared with cortical tissue from control individuals. Together, these studies indicate that *O*-GlcNAcylation regulates pathways critical for the maintenance of neuronal health and suggest that dysfunctional *O*-GlcNAc signaling may be an important contributor to neurodegenerative diseases.

O-GlcNAc | glycosylation | neurodegeneration | tau | amyloid beta

Despite the increasing prevalence of neurodegenerative diseases such as Alzheimer's disease (AD) and Parkinson's disease, there still are no effective treatments to prevent, cure, or stop neurons from degenerating. Neurodegeneration at the cellular level involves the dysfunction of several processes important for proper neuronal function and health, including synaptic plasticity (1), autophagy (2), mitochondrial dynamics (3), and cellular metabolism (4). An improved understanding of the protective factors responsible for maintaining neuronal health is essential for uncovering the biology of neuropathies and the development of more effective treatments for neurodegenerative conditions.

O-GlcNAc glycosylation (or *O*-GlcNAcylation) is a dynamic posttranslational modification that regulates important processes such as transcription (5, 6), proteostasis (7), the stress response (8), autophagy (9), and metabolism (6, 10). The *O*-GlcNAc transferase enzyme OGT catalyzes the covalent attachment of *N*-acetyl-D-glucosamine to serine or threonine residues of proteins, whereas β-*N*-acetylhexosaminidase (also known as "*O*-GlcNAcase," OGA) removes it (6). Although OGT is ubiquitously expressed, it is particularly abundant in neurons, where it is enriched in the nucleus (6) and at synapses (11). OGT participates in specialized neuronal processes, including activity-dependent transcription and long-term depression via regulation of cAMP-responsive element binding protein (CREB) (5) and the AMPA receptor GluA2 subunit (12), respectively. *O*-GlcNAcylation also has been implicated in neurodegenerative diseases and is reported on proteins such as amyloid precursor protein (APP) (13), α-synuclein (14), neurofilament M (NFM) (15), and tau (16). Several studies have suggested neuroprotective roles for the modification. For example, increasing global levels of *O*-GlcNAcylation in neurons decreased the production of pathological forms of NFM and tau (15, 16) and directly inhibited the aggregation of both tau (17) and α-synuclein (18). Glycosylation of nicastrin, a component of the

γ-secretase complex, enhanced the nonamyloidogenic processing of APP (13, 19). Moreover, raising *O*-GlcNAcylation levels by pharmacological inhibition of OGA attenuated amyloid-β deposition, tau phosphorylation, motor deficits, and memory impairments in certain AD mouse models (17, 19). On the other hand, studies also have suggested neurodegenerative roles for *O*-GlcNAcylation. For instance, increasing *O*-GlcNAcylation levels exacerbated neurodegenerative phenotypes of tauopathy, amyloid β-peptide, and polyglutamine expansion in *Caenorhabditis elegans* models, whereas decreasing *O*-GlcNAcylation levels rescued those phenotypes (20). Thus, it is unclear whether *O*-GlcNAcylation has neuroprotective or neurodegenerative functions and whether aberrant *O*-GlcNAc signaling plays a direct role in the induction of neuronal pathology in vivo.

Understanding the functions of *O*-GlcNAcylation in the mature brain and in neurodegenerative diseases has been complicated by the difficulty of knocking out the *ogt* gene. Because OGT is ubiquitously expressed and is essential for cell-cycle progression and proliferation (6), constitutive deletion of OGT in mice resulted in embryonic lethality, and neuron-specific OGT deletion using a Syn1-Cre transgene led to severe developmental defects, increased phosphorylation of tau, and early postnatal lethality (21). In this study, we produced a forebrain-specific OGT conditional knockout (OGT cKO) mouse to assess the effects of *O*-GlcNAc depletion on learning, memory, and neuronal function in adult mice. The mice were phenotypically normal at birth but at 2 mo of age developed signs of severe, progressive neurodegeneration, including loss of neurons, gliosis, increased

Significance

O-GlcNAcylation is an abundant posttranslational modification suggested to have both neuroprotective and neurodegenerative functions. Although previous studies on *O*-GlcNAc have illustrated its potential to modulate preexisting phenotypes in neurodegenerative animal models, the importance of *O*-GlcNAcylation in both the induction of neuropathology and the functioning of healthy adult neurons remained unclear. We generated a forebrain-specific *O*-GlcNAc transferase conditional knockout mouse and found that diminution of *O*-GlcNAc signaling induced progressive neurodegeneration in vivo, including pathogenic processing of tau and amyloid precursor protein, widespread neuronal death, gliosis, and memory loss. These results indicate that *O*-GlcNAcylation regulates pathways critical for neuronal health and survival and that modulating *O*-GlcNAc signaling may represent a neuroprotective strategy for neurodegenerative diseases.
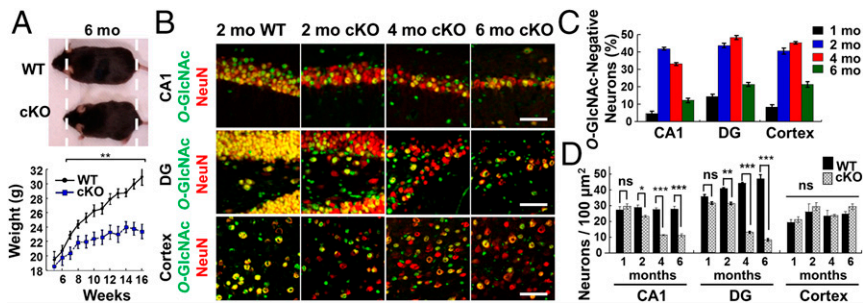
Fig. 1. Characterization of OGT knockout and neuronal loss. (*A*) OGT cKO mice were smaller than WT mice and displayed significantly reduced weight gain beginning at 7 wk. (*B*) An anti–*O*-GlcNAc antibody was used to image total *O*-GlcNAc levels (green) in hippocampal NeuN+ neurons (red). (*C*) Quantification of *O*-GlcNAc− neurons in the CA1, DG, and cortical regions. (*D*) Quantification of NeuN+ neurons illustrates neuronal loss in the CA1 and DG of OGT cKO mice. *$P < 0.05$, **$P < 0.005$, ***$P < 0.0005$. (Scale bars: 50 μm.)

hyperphosphorylated tau and Aβ−peptides, altered expression of genes involved in inflammation and cell-cycle arrest, and memory impairments. Together, our studies link OGT and diminished *O*-GlcNAcylation to the induction of neuropathological phenotypes and may have important implications for the study and treatment of neurodegenerative diseases.

Results

Generation of Forebrain-Specific OGT cKO Mice. We generated OGT cKO mice by crossing floxed *ogt* (OGTfl) mice (21) with αCamKII-Cre transgenic mice (22). Because the αCamKII-Cre transgene is expressed between postnatal day 14–21 in excitatory neurons in the postnatal forebrain, including the cortex, hippocampus, caudate nucleus, thalamus, and hypothalamus (22), this approach circumvents complications associated with OGT ablation during prenatal development. OGT cKO mice were produced at expected frequencies and were indistinguishable from their WT littermates at birth. However, they began to show a significant reduction in weight gain at 7 wk of age (11% at 7 wk and 32% at 16 wk) (Fig. 1*A*). Loss of OGT protein expression occurred in hippocampal CA1, dentate gyrus (DG), and cortical neurons and coincided with the time course of *O*-GlcNAc signal depletion (Fig. S1). Beginning at 1 mo of age, *O*-GlcNAcylation was undetectable with a pan-specific *O*-GlcNAc antibody in 5–15% of hippocampal CA1, DG, and cortical neurons (Fig. 1 *B* and *C*). By 2–4 mo, depletion of *O*-GlcNAcylation peaked in 30–50% of CA1, DG, and cortical neurons (Fig. 1*C*). By 6 mo, only 10–20% of the neurons lacked *O*-GlcNAc because of progressive neuronal death following OGT ablation. No change in OGT expression or *O*-GlcNAcylation levels was found in the cerebellum, which lacks αCaMKII-Cre transgene expression (Fig. S2). The observed forebrain-specific deletion of *ogt* was confirmed further by crossing the αCaMKII-Cre mice with RosaYFPfl mice (Fig. S2) and coincided well with previous examples of gene inactivation induced by the αCaMKII-Cre transgene (22).

Loss of *O*-GlcNAcylation in OGT cKO Mice Leads to Progressive Neurodegeneration. Loss of OGT was accompanied by a diminution in the overall brain size and a progressive, profound reduction in hippocampal and cortical neurons (Fig. 2*A*). Global changes in brain morphology were detectable by Nissl staining, which revealed a dramatic shrinkage of the hippocampus and cortex by 4 mo (Fig. 2*B*) and a significant decrease in cortical thickness at 4 and 6 mo (Fig. 2*C*). In the DG, a 23, 70, and 83% decrease in neuronal density was observed by neuronal nuclear antigen (NeuN) staining at 2, 4, and 6 mo, respectively (Fig. 1*D*). Similarly, neuronal loss was observed in the CA1 region of the hippocampus (20, 60, and 60% decrease in neuronal density at 2, 4, and 6 mo, respectively), although the cortical neuronal density did not change (Fig. 1*D*), likely because of the significant reduction in cortical thickness.

To evaluate the mechanism of neuronal death, we used TUNEL and Fluoro-Jade C (FJC) staining. The majority of DG neurons were TUNEL+ in 2-mo-old OGT cKO mice (Fig. 2*D*), demonstrating the presence of extensive apoptosis in the hippocampus. In addition, FJC staining revealed that more than 60% of DG neurons

had degenerated at 2 mo (Fig. 2*E*). FJC staining also was observed in the cortex, increasing fivefold from 2 mo to 4 mo of age (Fig. S2). In contrast, no detectable labeling of hippocampal neurons by TUNEL or FJC was observed in WT mice. Interestingly, although most FJC+ neurons lacked *O*-GlcNAcylation, some neighboring *O*-GlcNAc+ neurons were also FJC+ (arrowheads in Fig. 2*E*).

Increased Anxiety and Memory Impairments in OGT cKO Mice. To assess the functional consequences of conditional OGT knockout, we evaluated the mice in a series of behavioral tasks. At 5 mo of age, OGT cKO mice exhibited an excessive grooming phenotype and deficits in nest-making ability. In addition, OGT cKO mice displayed impaired exploratory behavior compared with WT mice
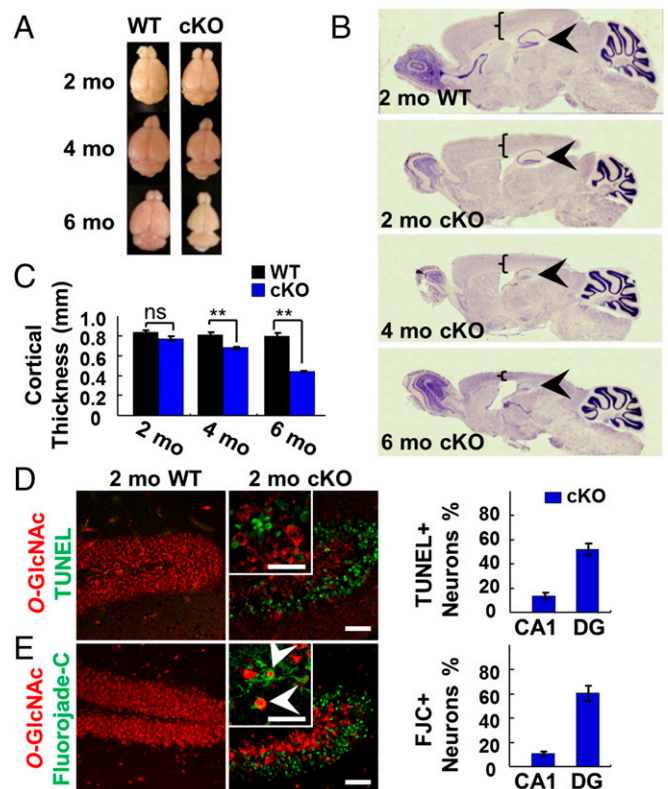

Fig. 2. OGT cKO mice displayed reduced brain size and neurodegeneration. (*A*) Overall brain size was reduced at 4 and 6 mo in OGT cKO mice. (*B* and *C*) Nissl staining showed shrinking of cortical (brackets) and hippocampal (arrowheads) structures in OGT cKO mice (*B*) along with significant decreases in cortical thickness (*C*). (*D*) Costaining for *O*-GlcNAc (red) and TUNEL (green) identified apoptotic neurons in the hippocampus of OGT cKO mice. (*E*) Costaining for *O*-GlcNAc (red) and FJC (green) identified degenerating neurons in the hippocampus of OGT cKO mice, some of which were positive for *O*-GlcNAc (arrowheads). **$P < 0.005$. (Scale bars: 50 μm.)
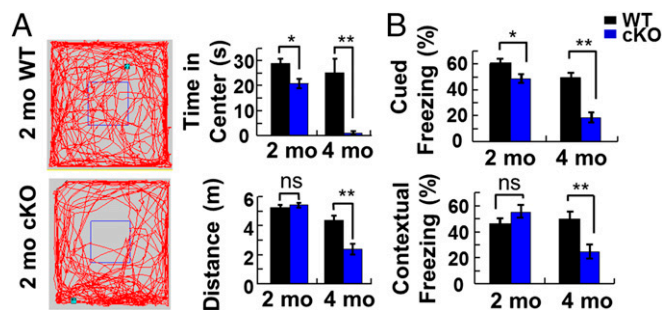
Fig. 3. Increased anxiety and impaired fear-related learning in OGT cKO mice. (*A*) In an open field test, OGT cKO mice showed a reduction in the time spent in the middle quadrant of the box and in the total distance traveled. (*B*) Deficits in cued fear conditioning were observed at 2 mo in OGT cKO mice, and deficits in both cued and contextual learning and memory were observed at 4 mo. $n = 12$ per group. $*P < 0.05$, $**P < 0.005$.

in an open field test, including a reduction in the time spent in the center of the field and the total distance traveled (Fig. 3*A*). Rotarod tests revealed no differences between OGT cKO and WT mice, suggesting that the differences in the open field test were caused by increased anxiety-like behaviors rather than by motor function defects (Fig. S3).

We also used a fear-conditioning paradigm to evaluate changes in the ability of OGT cKO mice to learn new associations. When tested 24 h after fear conditioning, the cKO mice displayed a small but significant deficit in amygdala-dependent cued freezing behavior at 2 mo but no change in hippocampus-dependent contextual freezing behavior (Fig. 3*B*). By 4 mo, however, significant deficits in both cued and contextual fear-related freezing behavior were observed (Fig. 3*B*). These results are consistent with the temporal pattern of neurodegeneration detected by histology and demonstrate a progressive impairment of fear-related associative learning and memory upon OGT depletion.

Up-Regulation of Immune-Response and Cell-Cycle–Related Genes.
To identify global transcriptional changes associated with the behavioral and histological phenotypes, we performed gene-expression microarray analyses. At 3 wk of age, only 10 differentially expressed genes were identified in the hippocampus of OGT cKO mice compared with WT mice, consistent with the minimal extent of OGT ablation and neuronal loss shown by histology (Fig. 1*D* and Table S1). In contrast, we observed a dramatic up-regulation of more than 900 genes in the hippocampus of 2-mo-old OGT cKO mice (Table S2). Among the most highly up-regulated genes were glial immune-response genes such as glial fibrillary acidic protein (*Gfap*), complement component 1q (*C1q*), and complement component 3 (*C3*). Increased expression of these and other representative genes was confirmed independently by quantitative RT-PCR (qRT-PCR) (Table S3). Notably, many of the same genes are up-regulated in established familial AD mouse models (Table S3) (23, 24). Furthermore, genes that showed little alteration in the AD mouse model Tg2576/PS-1$^{P264L/P264L}$, such as those encoding for GAP43, syntaxin, synaptophysin I, and synaptotagmin-I, were not differentially expressed in OGT cKO mice (Table S4) (23). Overall, the similarities in the transcriptional profiles between OGT cKO mice and AD mouse models suggest that they may share common underlying mechanisms of neurodegeneration.

To determine whether entire networks of genes were deregulated in OGT cKO mice, a weighted gene coexpression network analysis (WGCNA) was performed to organize genes into biologically meaningful groups. WGCNA identified two gene modules that were significantly correlated with OGT deletion [cor = 0.71 ($P = 3.8 \times 10^{-28}$ and cor = 0.77 ($P = 1.2 \times 10^{-18}$)] (Fig. S4). Using Gene Ontology analysis, we found that one

module was enriched with genes involved in the immune response ($P < 3.4 \times 10^{-4}$) such as Bcl-2 homologous antagonist killer (*Bak1*) and SH2-domain containing phosphatidylinositol-3,4,5-trisphosphate 5-phosphatase 2 (*Inppl1*). Bak1, a central pro-apoptotic member of the Bcl-2 family, is required for mitochondrial permeabilization and release of cytochrome *c* into the cytosol in the early stages of apoptosis (25). Enhanced expression of apoptosis- and immune-related genes is consistent with the extensive apoptosis (Fig. 2*D*) and gliosis (see Fig. 5*A*) observed in OGT cKO mice and with the up-regulation of immune-response genes observed in other AD mouse models (24). A second module was enriched with genes involved in cell-cycle arrest ($P < 3.8 \times 10^{-5}$), including antigen Ki-67 (*Mki67*), protein regulator of cytokinesis 1 (*Prc1*), and kinetochore protein Spc25 (*Spc25*) (Fig. S4).

To explore further the connection between OGT ablation and cell-cycle arrest, we probed OGT cKO mice for evidence of altered neuronal cell-cycle progression. Although immunostaining of hippocampal neurons for proliferating cell nuclear antigen (PCNA) and BrdU revealed no appreciable differences (Fig. S5), we observed a significant increase in the levels of cyclin A2 in OGT cKO mice compared with WT mice (Fig. 4*A*). Cyclin A2 is an initiator of DNA replication during S-phase and is a well-established marker for cell-cycle progression (26). Moreover, the protein expression levels of cyclin-dependent kinase 5 (CDK5), a negative regulator of cell-cycle progression, decreased significantly in OGT cKO mice compared with WT mice, as determined by Western blot analysis (Fig. 4*B*). Although there was no change in *CDK5* mRNA levels (Table S2), immunohistochemistry (IHC) analysis also indicated a specific reduction in CDK5 protein levels in *O*-GlcNAc–null hippocampal neurons (Fig. 4*C*), suggesting the potential for posttranscriptional regulation of CDK5 by *O*-GlcNAc. Taken together, these WGCNA, IHC, and Western blot analyses provide evidence of enhanced cell-cycle progression in the hippocampus of OGT cKO mice.

OGT cKO Mice Recapitulate Neurodegenerative Phenotypes. Gliosis, the activation of microglia and astrocytes, is associated with neuroinflammation and the pathology of neurodegenerative disease.
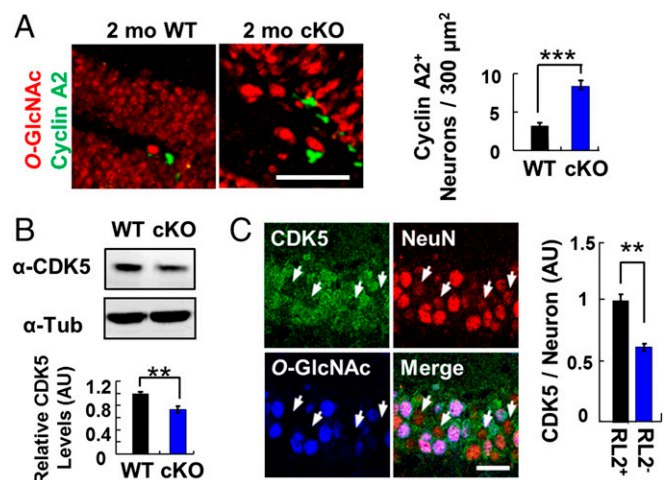

Fig. 4. Effects of *O*-GlcNAcylation on cell-cycle progression. (*A*) An increase in the number of Cyclin A2$^+$ neurons was observed by immunostaining in the DG of 2-mo-old OGT cKO mice relative to WT mice. $n = 4$. (Scale bar: 50 μm.) (*B*) A significant decrease in CDK5 expression levels was detected by Western blotting in the hippocampus of 2-mo-old OGT cKO mice. $n = 8$. (*C*) *O*-GlcNAc–negative neurons have decreased CDK5 immunostaining (arrowheads) in the hippocampus at 2 mo. CDK5 immunoreactivity was quantified in *O*-GlcNAc$^+$ (RL2$^+$) and *O*-GlcNAc$^-$ (RL2$^-$) neurons. $n = 4$. $**P < 0.005$, $***P < 0.0005$. (Scale bar: 10 μm.) AU, arbitrary units.

OGT cKO mice displayed extensive gliosis, consistent with the observed up-regulation of immune-response genes. The astrocyte marker GFAP and the microglial marker Iba-1 were significantly increased (6.5- and 14.9-fold, respectively) in the hippocampus of OGT cKO mice compared with WT mice beginning at 2 mo of age (Fig. 5A). By 4 mo, gliosis had spread to the cortex (Fig. S5) and was strongly correlated with the spatiotemporal loss of O-GlcNAcylation (Fig. 1C).

To determine whether OGT cKO mice displayed other neurodegenerative phenotypes, we investigated the levels of tau phosphorylation and aggregation. Phosphorylation of tau at Thr-205 and Thr-231 has been associated with paired-helical filamentous (PHF) tau oligomers, which aggregate to form neurofibrillary tangles (NFTs) (27). We observed increased tau phosphorylation at these sites (1.8- and 2.9-fold, respectively) in the mossy fibers and cell bodies of DG neurons in OGT cKO mice compared with WT mice (arrowheads in Fig. 5B). This result was confirmed further by Western blot analysis, which demonstrated a significant increase in phosphorylated tau (1.4-fold each for pSer-202/Thr-205 and pThr-231) (Fig. 5C) in the hippocampus of OGT cKO mice. Interestingly, although an inverse relationship between tau phosphorylation and O-GlcNAcylation has been observed (16, 17), the overall levels of tau O-GlcNAcylation at Ser-400 were not significantly decreased in the hippocampus of 2-mo-old OGT cKO mice compared with WT mice (Fig. S5). Because phosphorylation of tau at these sites has been linked to its aggregation, Thioflavin S was used to evaluate the presence of protein aggregates in the hippocampus. At 6 mo of age, OGT cKO mice displayed Thioflavin S⁺ protein deposits that were costained with a pThr-205 tau antibody (6.9-fold increase) (Fig. 5D and Fig. S5).

Soluble oligomeric Aβ-peptides, which are produced by the proteolytic processing of APP, have been shown to inhibit hippocampal LTP, disrupt cognitive function, and induce apoptosis (28). We observed a 6.8-fold increase in the level of the 42-mer Aβ-peptide and a 2.7-fold increase in the level of the 40-mer Aβ-peptide by ELISA in 6-mo-old OGT cKO mice compared with WT mice (Fig. 5E). Moreover, the ratio of 42/40-mer peptide increased by 2.5-fold, indicating enhanced accumulation of the more amyloidogenic 42-mer peptide (Fig. 5E) (28).

OGT Levels Are Decreased in Human AD Brains. In light of the marked neurodegenerative phenotypes of OGT cKO mice, we examined whether human AD brains had reduced levels of OGT expression at the cellular level. Previously, both increases and decreases in O-GlcNAcylated proteins had been reported in the cerebral cortex of AD brains compared with control individuals (29, 30). Notably, we found that cortical neurons from severe AD patients (Braak stage VI) displayed a 1.6-fold decrease in OGT protein levels compared with age- and sex-matched controls (Fig. 6), as revealed by IHC staining with an anti-OGT antibody. OGT protein levels in midstage AD patients (Braak stages IV and V) were also depleted, supporting the trend observed in severe AD patients, although the decrease was not statistically significant. These results demonstrate a correlation between lower OGT expression levels and the pathology of human neurodegeneration.

Discussion

In this study, we generated a forebrain-specific *ogt* cKO mouse to study the roles of O-GlcNAcylation in adult neurons. Because the mice survived to adulthood, the effects of *ogt* deletion on learning, memory, and adult neuronal function could be evaluated directly. Loss of OGT led to progressive neuronal death and other phenotypes associated with neurodegenerative diseases, including gliosis, activation of immune-response and cell-cycle genes, aberrant phosphorylation of tau, and amyloidogenic Aβ-42 peptides. OGT cKO mice also displayed behavioral deficits such as abnormal nesting behavior, memory impairments, and increased anxiety, which are characteristics observed in neurodegenerative mouse models of AD (31), obsessive-compulsive disorder (32), and schizophrenia (33). Notably, we found that human AD patients showed a significant decrease in OGT protein expression levels in the frontal cerebral cortex compared with control individuals, and this decrease correlated with progressive cognitive decline. Together, our studies reveal important neuroprotective roles for O-GlcNAcylation and suggest that alterations in O-GlcNAc signaling may contribute to neuronal pathology.

Both tau phosphorylation and APP processing were significantly altered in OGT cKO mice. Upon *ogt* deletion, we observed enhanced tau aggregation and hyperphosphorylation at sites associated with neurofibrillary tangles. These findings further support previous studies suggesting a reciprocal relationship between O-GlcNAc and phosphorylation on tau. For example, increasing global O-GlcNAc levels reduced tau phosphorylation at Ser-199, Thr-212, Thr-217, Ser-262, Ser-396, and Ser-422 in mouse brain slices (16). Moreover, inhibition of OGA elevated O-GlcNAc levels and decreased tau hyperphosphorylation in an AD mouse model (17). Although we observed no significant change in the levels of tau O-GlcNAcylated at Ser-400, it is possible that O-GlcNAcylation of tau is differentially regulated at specific sites
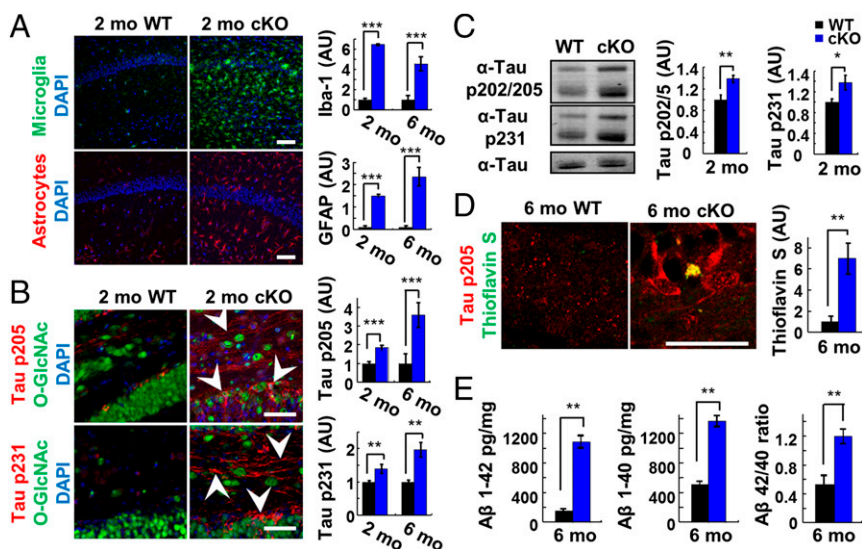

Fig. 5. OGT cKO mice exhibited neuroinflammation and increased phosphorylated tau and Aβ-peptide levels. (A, Left) Elevated expression of the neuroinflammatory markers Iba-1 (green) and GFAP (red) in the CA1 hippocampus of 2-mo-old OGT cKO mice compared with WT mice. (Right) Total pixel intensity from each field of view was quantified, and the mean ± SEM is shown. n = 4. (B) Phosphorylation of tau (pThr-205, pThr-231) increased and accumulated in both the soma and axons of DG neurons (arrowheads) of 2-mo-old OGT cKO mice. Quantification is shown at right. (C) Increased levels of tau phosphorylated at p202/205 and p231 in 2-mo-old OGT cKO mice, as revealed by Western blotting. n = 8. (D) Thioflavin S⁺ aggregates accumulated in 6-mo-old OGT cKO mice and were costained with phosphorylated tau (pThr-205). (E) The Aβ 42-mer and 40-mer peptide levels and the 42/40-mer peptide ratio increased in 6-mo-old OGT cKO mice, as quantified by ELISA. n = 4. *P < 0.05, **P < 0.005, ***P < 0.0005. (Scale bars: 50 μm in A and B; 10 μm in D.)
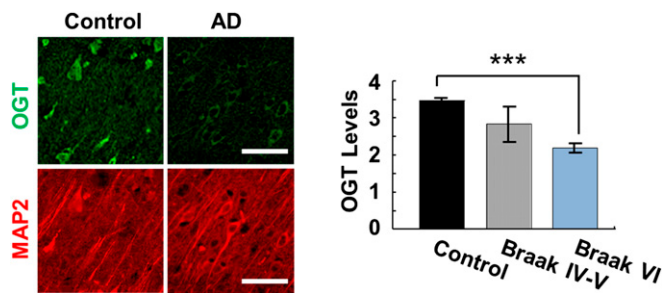
Fig. 6. Human AD brain tissue showed a significant reduction in OGT protein levels. (*Left*) The frontal cerebral cortex from AD patients was immunostained with an anti-OGT antibody (green) and with an anti-MAP2 antibody (red) as a control for neuronal number. (*Right*) A 1.6-fold reduction in neuronal OGT protein expression was observed in AD Braak stage VI patients (*n* = 8) compared with age- and sex-matched control individuals (*n* = 6). ***P < 0.0005. (Scale bars: 50 μm.)

or that a small amount of residual OGT may be sufficient to maintain *O*-GlcNAc levels at this site.

Previous studies have suggested that higher *O*-GlcNAcylation levels can enhance nonamyloidogenic processing of APP by raising α-secretase activity (13) and lowering γ-secretase activity (19). In accordance with these observations, we found that loss of OGT enhanced the pathological processing of APP in vivo, increasing the ratio of the amyloidogenic 42-mer Aβ-peptide to the 40-mer. Notably, accumulation of hyperphosphorylated tau and Aβ-peptides is not observed in many neurodegenerative mouse models, and the two phenotypes are rarely observed together. For example, 5XFAD mice that express five different familial AD mutations in APP and presenilin1 showed no accumulation of hyperphosphorylated tau (34), and mutant P301L tau transgenic mice displayed no increases in amyloid beta load (35) despite the presence of extensive neuronal death. Thus, the defects in tau phosphorylation and APP processing observed in OGT cKO mice are not likely to be indirect effects caused by a global requirement for OGT in proper neuronal function and survival. Together, the findings suggest that the *O*-GlcNAc modification plays a central role in regulating both APP and tau and that dysfunctional *O*-GlcNAc signaling may contribute to improper APP processing and tau pathology.

We performed gene microarray analyses to obtain insights into the global, systems-level changes induced by loss of OGT. Our studies revealed that several cell-cycle genes, including *Mki67*, *Prc1*, and *Spc25*, were up-regulated in OGT cKO mice. Consistent with an important role for OGT in cell-cycle regulation, *O*-GlcNAcylation previously has been shown to modulate cell-cycle progression by prolonging cyclin A and B expression and catalyzing proteolytic maturation of the critical cell-cycle regulator, host cell factor-1 (HCF-1) (36, 37). Interestingly, several genes involved in controlling oxidative stress were also significantly up-regulated in OGT cKO mice, including heme oxygenase 1 (*Hmox1*), cyclooxygenase 1 (*Ptgs1*), and activity-dependent neuroprotective protein homeobox 2 (*ADNP2*). *O*-GlcNAcylation previously has been shown to be required for stress granule assembly in response to oxidative stress and to decrease oxidative stress in cardiomyocytes by reducing reactive oxygen species (8, 38). Thus, one important mechanism by which OGT may exert its neuroprotective effects is through the regulation of critical cell-cycle regulators and modulators of oxidative stress. The two-hit hypothesis of AD postulates that both oxidative stress and mitotic dysregulation are necessary and sufficient to cause the neurodegeneration associated with AD (39). Further supporting the gene-expression analyses, we found that cyclin A2, a marker of cell-cycle progression, was increased in OGT cKO mice, providing strong evidence for enhanced cell-cycle progression in the hippocampi of these mice. Moreover, CDK5 protein expression levels were significantly decreased upon loss of OGT. CDK5 represses neuronal cell-cycle

advancement (40) and is an important upstream regulator of oxidative stress through phosphorylation of peroxiredoxin I/II and p53 (39). Interestingly, a recent paper suggests that blocking *O*-GlcNAcylation of CDK5 can lead to neuronal apoptosis by enhancing its association with the p53 pathway (41). Several other studies have implicated aberrant cell-cycle advancement in AD-associated neurodegeneration through deregulation of CDK5 levels and activity (40, 42). Together, these results suggest that a major mode by which OGT ablation leads to neurodegeneration is through cell-cycle dysfunction. Future studies will focus on understanding the detailed mechanisms by which OGT affects CDK5 function, the cell cycle, and oxidative stress in neurons.

Lagerlöf et al. reported that the tamoxifen-induced deletion of *ogt* from αCaMKII⁺ neurons in adult mice leads to obesity caused by overeating (43). This phenotype was the result of reduced satiety caused by OGT ablation in the paraventricular nucleus (PVN) of the hypothalamus. Interestingly, no change in neuronal number in the hippocampus or PVN was noted upon quantification of DAPI⁺ cells, although the age of the mice analyzed was not reported. There could be several explanations for the phenotypic differences between Lagerlöf's model and ours. First, there likely are differences in the timing of the OGT knockout in the αCaMKII-Cre versus the αCaMKII-CreER^T2 tamoxifen-inducible systems. In our study, loss of OGT and *O*-GlcNAcylation began at 4 wk of age, and the neuronal loss and degenerative phenotypes were not significant until 8 wk of age. In the Lagerlöf study, tamoxifen injections were initiated at 6 wk of age, and phenotypic responses were monitored up to 4 wk later. Second, it is possible that the neurodegenerative phenotypes were not yet apparent during the window of their study, because tamoxifen-induced Cre recombination can take several days. Furthermore, variability in the location and timing of αCaMKII promoter-driven Cre recombination has been described previously and attributed to differences in the location of αCaMKII-Cre transgene insertion within the genome (44). Alternatively, excitatory forebrain neurons may be more vulnerable to OGT deletion at specific stages of maturation. Last, any effects on satiety in our model were likely obscured by the strong neurodegenerative phenotype. The phenotypic differences between the two OGT cKO models suggest that OGT plays specific roles in neuronal health and homeostasis during various stages, and they underscore the importance of the precise spatiotemporal coordination of *O*-GlcNAcylation.

The *O*-GlcNAc modification appears to play multiple, complex roles in neurodegeneration, and previous studies paradoxically have suggested that decreasing *O*-GlcNAcylation has both neuroprotective and neurodegenerative effects (17, 20). We show that loss of *O*-GlcNAcylation in healthy neurons leads to progressive neurodegeneration in vivo, providing strong evidence that *O*-GlcNAc has neuroprotective functions in adult mammalian neurons. The neurodegenerative, transcriptional, and behavioral phenotypes observed in OGT cKO mice are shared by many AD mouse models, suggesting common mechanisms of neurodegeneration. It is noteworthy that loss of OGT alone is sufficient to induce neurodegenerative pathologies and that this neurodegeneration occurs relatively rapidly. Induction of such phenotypes in other mouse models generally requires mutation or overexpression of multiple familial AD-related proteins such as tau, APP, and presenilin (31), and the pathological phenotypes take 9–12 mo to progress (23, 31). The rapid course of neurodegeneration in OGT cKO mice underscores the critical importance of OGT in the maintenance of adult neuronal health and suggests that dysfunctional *O*-GlcNAc signaling may be an important contributor to neuronal pathology. Collectively, our studies provide a direct link between the ablation of *O*-GlcNAcylation and the induction of neurodegenerative phenotypes, suggesting that strategies to control *O*-GlcNAcylation and its neuroprotective effects may represent an approach for the treatment of neurodegenerative conditions.

Methods

Human Tissue. Brain samples of frontal cortex from control ($n = 6$), Braak stage VI ($n = 8$), and Braak stage IV-V ($n = 4$) patients were obtained from the Alzheimer's Disease Research Center at the University of California, Los Angeles. Samples were from patients with a similar age, sex, and postmortem interval.

Mice. αCaMKII-Cre mice were provided by Mary Kennedy, California Institute of Technology, Pasadena, CA (22), and OGTfl mice (B6.129-Ogttm1Gwh/J) were purchased from Jackson Laboratories. Both lines were backcrossed six times into the C57/Bl6 background. Details of breeding are provided in *SI Methods*. All animal procedures were performed in accordance with the NIH Guide for the Care and Use of Laboratory Animals and approved by the Institutional Animal Care and Use Committee of the California Institute of Technology.

IHC. Mice were transcardially perfused with 4% (wt/vol) paraformaldehyde (PFA) and were fixed overnight in 4% (wt/vol) PFA at 4 °C, followed by cryoprotection with 15–30% (wt/vol) sucrose. Sagittal sections (20 μm) were obtained using a Leica CM1850 cryostat and were stored in an ethylene glycol solution at −20 °C. Slices were stained with primary antibody in 2% (vol/vol) goat serum, 0.1% Triton-X 100 in PBS overnight at 4 °C. Slices were mounted with Vectashield (Vector Labs, H1200), coded, and imaged with a Zeiss 700 confocal microscope, with the investigator blind to the genotype. Images were collected from slices spaced 100 μm apart through the region of interest. A minimum of 12 slices were quantified for each animal, and a minimum of four animals were evaluated for each genotype. Quantification of fluorescence intensity was performed as previously described (45) and was analyzed using a two-tailed, unpaired Student's t test.

Additional materials and methods, including detailed IHC procedures, behavioral experiments, ELISA, microarray, and qRT-PCR analyses, are provided in *SI Methods*. A list of primers used in this study can be found in Table S5.

1. Palop JJ, Mucke L (2010) Amyloid-beta-induced neuronal dysfunction in Alzheimer's disease: From synapses toward neural networks. *Nat Neurosci* 13(7):812–818.
2. Wong E, Cuervo AM (2010) Autophagy gone awry in neurodegenerative diseases. *Nat Neurosci* 13(7):805–811.
3. Chen H, Chan DC (2009) Mitochondrial dynamics–fusion, fission, movement, and mitophagy–in neurodegenerative diseases. *Hum Mol Genet* 18(R2):R169–R176.
4. Mosconi L (2005) Brain glucose metabolism in the early and specific diagnosis of Alzheimer's disease. FDG-PET studies in MCI and AD. *Eur J Nucl Med Mol Imaging* 32(4):486–510.
5. Rexach JE, et al. (2012) Dynamic O-GlcNAc modification regulates CREB-mediated gene expression and memory formation. *Nat Chem Biol* 8(3):253–261.
6. Hart GW, Slawson C, Ramirez-Correa G, Lagerlof O (2011) Cross talk between O-GlcNAcylation and phosphorylation: Roles in signaling, transcription, and chronic disease. *Annu Rev Biochem* 80:825–858.
7. Hanover JA, Wang P (2013) O-GlcNAc cycling shows neuroprotective potential in C. elegans models of neurodegenerative disease. *Worm* 2(4):e27043.
8. Ngoh GA, Watson LJ, Facundo HT, Jones SP (2011) Augmented O-GlcNAc signaling attenuates oxidative stress and calcium overload in cardiomyocytes. *Amino Acids* 40(3):895–911.
9. Guo B, et al. (2014) O-GlcNAc-modification of SNAP-29 regulates autophagosome maturation. *Nat Cell Biol* 16(12):1215–1226.
10. Yi W, et al. (2012) Phosphofructokinase 1 glycosylation regulates cell growth and metabolism. *Science* 337(6097):975–980.
11. Cole RN, Hart GW (2001) Cytosolic O-glycosylation is abundant in nerve terminals. *J Neurochem* 79(5):1080–1089.
12. Taylor EW, et al. (2014) O-GlcNAcylation of AMPA receptor GluA2 is associated with a novel form of long-term depression at hippocampal synapses. *J Neurosci* 34(1):10–21.
13. Jacobsen KT, Iverfeldt K (2011) O-GlcNAcylation increases non-amyloidogenic processing of the amyloid-β precursor protein (APP). *Biochem Biophys Res Commun* 404(3):882–886.
14. Morris M, et al. (2015) Tau post-translational modifications in wild-type and human amyloid precursor protein transgenic mice. *Nat Neurosci* 18(8):1183–1189.
15. Lüdemann N, et al. (2005) O-glycosylation of the tail domain of neurofilament protein M in human neurons and in spinal cord tissue of a rat model of amyotrophic lateral sclerosis (ALS). *J Biol Chem* 280(36):31648–31658.
16. Liu F, Iqbal K, Grundke-Iqbal I, Hart GW, Gong CX (2004) O-GlcNAcylation regulates phosphorylation of tau: A mechanism involved in Alzheimer's disease. *Proc Natl Acad Sci USA* 101(29):10804–10809.
17. Yuzwa SA, et al. (2012) Increasing O-GlcNAc slows neurodegeneration and stabilizes tau against aggregation. *Nat Chem Biol* 8(4):393–399.
18. Marotta NP, et al. (2015) O-GlcNAc modification blocks the aggregation and toxicity of the protein α-synuclein associated with Parkinson's disease. *Nat Chem* 7(11):913–920.
19. Kim C, et al. (2013) O-linked β-N-acetylglucosaminidase inhibitor attenuates β-amyloid plaque and rescues memory impairment. *Neurobiol Aging* 34(1):275–285.
20. Wang P, et al. (2012) O-GlcNAc cycling mutants modulate proteotoxicity in Caenorhabditis elegans models of human neurodegenerative diseases. *Proc Natl Acad Sci USA* 109(43):17669–17674.
21. O'Donnell N, Zachara NE, Hart GW, Marth JD (2004) Ogt-dependent X-chromosome-linked protein glycosylation is a requisite modification in somatic cell function and embryo viability. *Mol Cell Biol* 24(4):1680–1690.
22. Schweizer C, et al. (2003) The gamma 2 subunit of GABA(A) receptors is required for maintenance of receptors at mature synapses. *Mol Cell Neurosci* 24(2):442–450.
23. Dickey CA, et al. (2003) Selectively reduced expression of synaptic plasticity-related genes in amyloid precursor protein + presenilin-1 transgenic mice. *J Neurosci* 23(12):5219–5226.
24. Wu Z-L, et al. (2006) Comparative analysis of cortical gene expression in mouse models of Alzheimer's disease. *Neurobiol Aging* 27(3):377–386.
25. Tait SW, Green DR (2010) Mitochondria and cell death: Outer membrane permeabilization and beyond. *Nat Rev Mol Cell Biol* 11(9):621–632.
26. Gong D, Ferrell JE, Jr (2010) The roles of cyclin A2, B1, and B2 in early and late mitotic events. *Mol Biol Cell* 21(18):3149–3161.
27. Hanger DP, Anderton BH, Noble W (2009) Tau phosphorylation: The therapeutic challenge for neurodegenerative disease. *Trends Mol Med* 15(3):112–119.
28. LaFerla FM, Green KN, Oddo S (2007) Intracellular amyloid-beta in Alzheimer's disease. *Nat Rev Neurosci* 8(7):499–509.
29. Liu F, et al. (2009) Reduced O-GlcNAcylation links lower brain glucose metabolism and tau pathology in Alzheimer's disease. *Brain* 132(Pt 7):1820–1832.
30. Förster S, et al. (2014) Increased O-GlcNAc levels correlate with decreased O-GlcNAcase levels in Alzheimer disease brain. *Biochim Biophys Acta* 1842(9):1333–1339.
31. Oddo S, et al. (2003) Triple-transgenic model of Alzheimer's disease with plaques and tangles: Intracellular Abeta and synaptic dysfunction. *Neuron* 39(3):409–421.
32. Welch JM, et al. (2007) Cortico-striatal synaptic defects and OCD-like behaviours in Sapap3-mutant mice. *Nature* 448(7156):894–900.
33. Lijam N, et al. (1997) Social interaction and sensorimotor gating abnormalities in mice lacking Dvl1. *Cell* 90(5):895–905.
34. Oakley H, et al. (2006) Intraneuronal β-amyloid aggregates, neurodegeneration, and neuron loss in transgenic mice with five familial Alzheimer's disease mutations: Potential factors in amyloid plaque formation. *J Neurosci* 26(40):10129–10140.
35. Götz J, Chen F, van Dorpe J, Nitsch RM (2001) Formation of neurofibrillary tangles in P301l tau transgenic mice induced by Abeta 42 fibrils. *Science* 293(5534):1491–1495.
36. Slawson C, et al. (2005) Perturbations in O-linked β-N-acetylglucosamine protein modification cause severe defects in mitotic progression and cytokinesis. *J Biol Chem* 280(38):32944–32956.
37. Capotosti F, et al. (2011) O-GlcNAc transferase catalyzes site-specific proteolysis of HCF-1. *Cell* 144(3):376–388.
38. Ohn T, Kedersha N, Hickman T, Tisdale S, Anderson P (2008) A functional RNAi screen links O-GlcNAc modification of ribosomal proteins to stress granule and processing body assembly. *Nat Cell Biol* 10(10):1224–1231.
39. Herrup K, Yang Y (2007) Cell cycle regulation in the postmitotic neuron: Oxymoron or new biology? *Nat Rev Neurosci* 8(5):368–378.
40. Zhang J, et al. (2008) Nuclear localization of Cdk5 is a key determinant in the post-mitotic state of neurons. *Proc Natl Acad Sci USA* 105(25):8772–8777.
41. Ning X, et al. (June 17, 2016) The O-GlcNAc modification of CDK5 involved in neuronal apoptosis following in vitro intracerebral hemorrhage. *Cell Mol Neurobiol*, 10.1007/s10571-016-0391-y.
42. Zhang J, Li H, Zhou T, Zhou J, Herrup K (2012) Cdk5 levels oscillate during the neuronal cell cycle: Cdh1 ubiquitination triggers proteosome-dependent degradation during S-phase. *J Biol Chem* 287(31):25985–25994.
43. Lagerlöf O, et al. (2016) The nutrient sensor OGT in PVN neurons regulates feeding. *Science* 351(6279):1293–1296.
44. Tsien JZ, et al. (1996) Subregion- and cell type-restricted gene knockout in mouse brain. *Cell* 87(7):1317–1326.
45. Zhang X, et al. (2005) A potent small molecule inhibits polyglutamine aggregation in Huntington's disease neurons and suppresses neurodegeneration in vivo. *Proc Natl Acad Sci USA* 102(3):892–897.
46. Southwell AL, Ko J, Patterson PH (2009) Intrabody gene therapy ameliorates motor, cognitive, and neuropathological symptoms in multiple mouse models of Huntington's disease. *J Neurosci* 29(43):13589–13602.
47. Haubensak W, et al. (2010) Genetic dissection of an amygdala microcircuit that gates conditioned fear. *Nature* 468(7321):270–276.
48. Wojtowicz JM, Kee N (2006) BrdU assay for neurogenesis in rodents. *Nat Protoc* 1(3):1399–1405.
49. Schmittgen TD, Livak KJ (2008) Analyzing real-time PCR data by the comparative C(T) method. *Nat Protoc* 3(6):1101–1108.
50. Dudoit S, Yang Y, Callow M, Speed T (2002) Statistical methods for identifying differentially expressed genes in replicated cDNA microarray experiments. *Stat Sin* 12:111–139.
51. Langfelder P, Horvath S (2008) WGCNA: An R package for weighted correlation network analysis. *BMC Bioinformatics* 9:559.
52. Carlson M (2016) GO.db: A set of annotation maps describing the entire Gene Ontology. R package version 3.4.0. Available at https://bioconductor.org/packages/release/data/annotation/html/GO.db.html. Accessed November 11, 2016.
53. Hu Z, et al. (2013) VisANT 4.0: Integrative network platform to connect genes, drugs, diseases and therapies. *Nucleic Acids Res* 41(Web Server issue):W225-31.

NEUROSCIENCE